Environmental Toxicology and Chemistry—Volume 37, Number 2—pp. 538–550, 2018
Received: 27 April 2017 | Revised: 17 June 2017 | Accepted: 28 September 2017

Environmental Toxicology

Chronic Exposure of a Freshwater Mussel to Elevated pCO_2: Effects on the Control of Biomineralization and Ion-Regulatory Responses

Jennifer D. Jeffrey,[a,*] Kelly D. Hannan,[a,b] Caleb T. Hasler,[a,c] and Cory D. Suski[a]

[a]Department of Natural Resources and Environmental Science, University of Illinois at Urbana–Champaign, Urbana, Illinois, USA
[b]ARC Centre of Excellence for Coral Reef Studies, James Cook University, Townsville, Australia
[c]Department of Biology, University of Winnipeg, Winnipeg, Manitoba, Canada

Abstract: Freshwater mussels may be exposed to elevations in mean partial pressure of carbon dioxide (pCO_2) caused by both natural and anthropogenic factors. The goal of the present study was to assess the effects of a 28-d elevation in pCO_2 at 15 000 and 50 000 μatm on processes associated with biomineralization, ion regulation, and cellular stress in adult *Lampsilis siliquoidea* (Barnes, 1823). In addition, the capacity for mussels to compensate for acid-base disturbances experienced after exposure to elevated pCO_2 was assessed over a 14-d recovery period. Overall, exposure to 50 000 μatm pCO_2 had more pronounced physiological consequences compared with 15 000 μatm pCO_2. Over the first 7 d of exposure to 50 000 μatm pCO_2, the mRNA abundance of chitin synthase (*cs*), calmodulin (*cam*), and calmodulin-like protein (*calp*) were significantly affected, suggesting that shell formation and integrity may be altered during pCO_2 exposure. After the removal of the pCO_2 treatment, mussels may compensate for the acid-base and ion disturbances experienced during pCO_2 exposure, and transcript levels of some regulators of biomineralization (carbonic anhydrase [*ca*], *cs*, *cam*, *calp*) as well as ion regulation (na^+-k^+-adenosine triphosphatase [*nka*]) were modulated. Effects of elevated pCO_2 on heat shock protein 70 (*hsp70*) were limited in the present study. Overall, adult *L. siliquoidea* appeared to regulate factors associated with the control of biomineralization and ion regulation during and/or after the removal of pCO_2 exposure. *Environ Toxicol Chem* 2018;37:538–550. © 2017 SETAC

Keywords: Chitin synthase; Na^+-K^+-ATPase; Calmodulin; Mollusk toxicology; Freshwater toxicology; Benthic macroinvertebrates

INTRODUCTION

Freshwater ecosystems may experience an increase in the mean partial pressure of carbon dioxide (pCO_2) for a variety of reasons, including climate change [1], deforestation [2], agricultural and urban activities [3], and invasive species management [4]. Natural variations in the pCO_2 of freshwater systems also occur at a local and global scale, with mean CO_2 levels that can range from 647 to 38 000 μatm globally and that fluctuate seasonally [5]. As a result of the natural and anthropogenic sources of change in freshwater pCO_2, it becomes important to understand the potential consequences for freshwater biota; however, at present our understanding of these consequences is limited [6]. Research into the impacts of elevations in aquatic pCO_2 has largely focused on marine systems because of the well-characterized acidification of oceanic systems with increasing atmospheric CO_2 [7]. For marine biota, physiological and behavioral alterations have been observed in a range of organisms [8–10]. Importantly, changes in seawater chemistry and carbonate saturation have resulted in reduced calcification and growth rates in marine calcifying organisms such as bivalves [9]. Therefore, similar negative consequences might be expected for freshwater bivalves if environmental pCO_2 should rise.

In freshwater systems, unionid mussels provide a number of important ecological functions such as water filtration, generation of nutrient-rich areas, and food sources for other animals [11]; nevertheless, anthropogenic alterations to their habitats have resulted in their decline, making them one of most imperiled taxa in North America [12]. Moreover, because of their limited mobility, freshwater mussels may be acutely sensitive to environmental disturbances such as elevations in pCO_2. In addition to other potential natural and anthropogenic sources [6], populations of freshwater mussels in the upper Midwest

* Address correspondence to jjeffrey@illinois.edu
Published online 2 October 2017 in Wiley Online Library (wileyonlinelibrary.com).
DOI: 10.1002/etc.3991

of the USA may be at risk of future exposures to elevated pCO_2 because zones of elevated CO_2 are being considered as a potential control mechanism to deter the movements of bigheaded carp (i.e., silver carp *Hypophthalmichthys molitrix* and bighead carp *H. nobilis*) [13]. This barrier would consist of artificially elevating pCO_2 up to 100 times greater than ambient conditions in localized areas (Cupp et al. [14] and Donaldson et al. [15]), where the threat of carp invasion is high. The potential exposure to these extreme levels of CO_2 provides an opportunity to study the responses of freshwater mussels to elevations in pCO_2, an area that has until recently been poorly investigated [16–20], providing a framework for understanding the physiological and ecological impacts of natural and anthropogenic increases in pCO_2 on threatened freshwater mussel populations.

The exposure of mussels to elevations in pCO_2 results in the acidification of intracellular and extracellular fluids, which can lead to a host of physiological and ecological consequences. In unionid mussels, hemolymph has a limited buffering capacity, no respiratory pigments, and a low osmotic concentration, and mussels rely on the bicarbonate-carbonate buffer system to at least, in part, respond to acidosis [21]. In response to acidosis, hemolymph HCO_3^- (as well as Ca^{2+}) levels increase as $CaCO_3$ is released from the shell [22]. The same bicarbonate buffering system is necessary for $CaCO_3$ crystal formation for shell deposition through the reverse reaction, and this process is dependent on the maintenance of extrapallial fluid (fluid in contact with the inner shell surface) pH by the removal of H^+ [23,24]. Thus, formation of the shell can be compromised in high pCO_2 environments as a result of alterations in the speciation of the carbonate system of the hemolymph and extrapallial fluid, and because of the utilization of $CaCO_3$ stores from the shell (i.e., source of HCO_3^-) for acid-base regulation, as has been shown in marine bivalves (Melzner et al. [25] and Michaelidis et al. [26]). Overall, the link between acid-base regulation and calcification of the shell may result in negative consequences for freshwater mussel shell integrity and growth in high pCO_2 environments, which may lead to ultimate decreases in survival and further population declines.

As a result of the intricate link between the transport of substrates for $CaCO_3$ crystal formation and acid-base and ion-regulatory processes in mussels, exposure to elevated pCO_2 may have consequences for the biological control of calcification and ion homeostasis. Biomineralization related to shell formation is a highly controlled and energetically expensive process [23]. The formation of the shell is controlled by a suite of regulators including chitin synthase (CS), carbonic anhydrase (CA), calmodulin (CaM), and CaM-like protein, and these regulators have been shown to be modulated by elevated pCO_2 exposure in marine and/or freshwater bivalves [19,27–29]. In addition, acid-base regulation during pCO_2 exposure resulted in ionic disturbances (e.g., changes in hemolymph Ca^{2+}, Na^+, Cl^-, and HCO_3^- levels) in several freshwater mussel species [16–18], presumably caused by the role of the Na^+/H^+ exchanger and the Cl^-/HCO_3^- anion exchanger in H^+ excretion and HCO_3^- retention, respectively. As an important regulator of secondary active ion transport, Na^+-K^+-adenosine triphosphatase (NKA) provides the driving force necessary for these acid-base and ion-regulatory responses, and may thus be sensitive to changes in environmental pCO_2. In addition to biomineralization and acid-base responses, regulators of cellular stress such as heat shock protein 70 (HSP70) have been suggested as biomarkers of stress in response to changes in freshwater [19] and marine [30] pCO_2. Overall, these physiological responses to elevated pCO_2 are energetically demanding and, as a result, freshwater mussels may experience reduced survival and stress coping because of increased environmental pCO_2.

Thus far, studies suggest that exposure to elevated pCO_2 results in changes in hemolymph ion concentrations in adult freshwater mussels, likely caused by acid-base regulatory responses [16–18], and mussels may recover, at least in part, once the CO_2 stressor is removed [16]. Furthermore, biological control of shell formation in adult freshwater mussels (i.e., *cs* mRNA) [19] and shell growth in juvenile mussels [20] were affected by long-term pCO_2 exposure ($>$ 28 d), and normal shell growth may resume post-CO_2 exposure [20]. Overall, however, the mechanisms underlying the observed physiological responses to exposure to elevations in pCO_2 remain poorly understood. With the possibility that freshwater pCO_2 may rise in the future because of natural or anthropogenic factors, an increased understanding of the physiological mechanisms utilized by mussels to respond to elevated pCO_2 will help to define how mussel individuals and populations may be impacted in the future [6]. Consequently, the goals of the present study were to quantify, at a molecular level: 1) effects of a sustained increase in pCO_2 on freshwater mussels, and 2) potential for mussels to recover from disturbances following the removal of the CO_2 stressor by assessing regulators of biomineralization, ion-regulatory responses, and cellular-stress responses. To accomplish these goals, adult *Lampsilis siliquoidea* (Barnes, 1823) were exposed to either 15 000 or 50 000 μatm pCO_2 for up to 28 d, representing scenarios in which mussels may be exposed to elevated pCO_2 at a location close to the deployment of a CO_2 barrier (50 000 μatm), or downstream of the barrier application area (15 000 μatm) where water pCO_2 would have dissipated to some extent. Because of their limited mobility, it is possible that mussels could experience elevations in pCO_2 for an extended period similar to that used in the present study; however, if mussels were relocated away from areas of CO_2 infusion for conservation purposes, or if exposures were intermittent [18], mussels may also be provided with the opportunity to recover from pCO_2 exposure. Thus, a recovery period of up to 14 d was evaluated after the period of pCO_2 exposure. Gene expression patterns of *cs*, *ca*, *cam*, *calp*, *nka*, and *hsp70* were assessed in the gill and/or mantle of mussels, representing candidates for the control of biomineralization, ion-regulatory responses, and the stress response. The approach used in the present study provides an opportunity to assess, at the organismal level, how mussels respond to elevations in pCO_2, providing a framework for a greater understanding of the mechanisms underlying potential population level responses of freshwater mussels in high pCO_2 environments.

MATERIALS AND METHODS

Experimental animals

Adult *L. siliquoidea* ($n = 138$, length 65.5 ± 0.5 mm, mean ± standard error [SE]) were obtained from a captive propagation program at Missouri State University, Springfield, MO, and held at the Aquatic Research Facility at the University of Illinois, Urbana–Champaign, IL, as in Hannan et al. [16]. Mussels were measured for size (length, width, and depth) using digital calipers (Fisher Scientific) and tagged for identification using Queen Marking Kit tags (The Bee Works). Mussels were distributed evenly among 3 recirculating holding systems and were held for at least 1 wk before experimentation, at which time each holding system was assigned to a pCO_2 treatment (i.e., one replicate per treatment, see section *Chronic pCO_2 exposure*). Each holding system consisted of a 128.7-L tank ($82.6 \times 42.5 \times 47.0$ cm) for holding mussels that contained sediment (5 cm of sand; Old Castle all-purpose sand). Holding systems were supplied with water from a 0.04-ha natural earthen-bottom pond with ample vegetation that overflowed from the holding tank into a reservoir and was pumped back into the holding tank, creating a closed recirculating system. Each holding system was equipped with a Teco 500 aquarium heater/chiller (TECO-US; Aquarium Specialty) to maintain water temperatures and a low-pressure air blower (Sweetwater; SL24H Pentair) for aeration. Water changes of 50% were performed weekly to maintain water quality, and water quality was assessed daily. During the pre-exposure period, dissolved oxygen (7.84 ± 0.17 mg/L) and temperature (21.1 ± 0.1 °C) were recorded with a portable meter (YSI 550A; Yellow Springs Instruments). Water pH (8.42 ± 0.03) and alkalinity (188 ± 3 mg/L $CaCO_3$) were measured using a handheld meter (WTW; pH 3310 meter) calibrated regularly and a digital titration kit (Titrator model 16 900, cat. no. 2271900; Hach), respectively. Concentrations of CO_2 (5.5 ± 0.2 mg/L) were quantified using a CO_2 titration kit (Hach; catalog no. 2272700). In addition to the naturally occurring sources that would be present in the pond water, mussels were fed a commercial shellfish diet every other day consisting of algae species ranging in particle sizes (Shellfish Diet 1800, Nanno 3600, Instant Algae; Reed Mariculture). Mussel tanks were carefully monitored for the clearance of algae from the water, to ensure that food availability was not restricted. Mussels did not receive food 24 h before sampling.

Chronic pCO_2 exposure

As part of the chronic pCO_2 exposure, mussels were exposed to one of 3 treatments: control conditions (< 100 μatm pCO_2), approximately 15 000 μatm pCO_2, or approximately 50 000 μatm pCO_2 for up to 28 d. Fish have been shown to avoid pCO_2 of approximately 30 000 to 50 000 μatm (60–70 mg/L) [14,15]; thus levels of this magnitude or higher (to ensure 100% effectiveness) were considered for the highest concentrations used in the present study. The intermediate concentration of 15 000 μatm might be expected should freshwater rivers experience an approximately 1.5 to 15 times increase in current CO_2 levels [5]. For the control group, pCO_2 levels remained unaltered for the duration of the experiment (< 100 μatm, the lowest detectable limit of the CO_2 probe). Target CO_2 levels were maintained with a pH controller (PINPOINT; American Marine) that added compressed CO_2 gas (commercial grade, 99.9% purity) into the system through an air stone if the pH rose above a target level [31]. Water pCO_2 was monitored throughout the exposure period using a modified infrared probe (Vaisala GMP220 and GMT221; Table 1). The concentration of CO_2, temperature, dissolved oxygen, pH, and alkalinity were also monitored daily as described earlier (Table 1). After 28 d of exposure to elevated pCO_2, a set of mussels was also moved to control conditions (< 100 μatm) for up to 14 d to quantify recovery from pCO_2 exposure.

Mussels were terminally sampled following 1, 4, 7, or 28 d of pCO_2 exposure, or 7 or 14 d after their return to control conditions ($n = 7$–8 at each time point). Size (length, width, and depth) was determined using digital calipers. Mussels were sampled for mantle (consisted of a combination of mantle edge, center, and pallial regions) and gill, and tissues were placed in 1 mL of RNAlater Stabilization Solution (Ambion, catalog no. AM7020; ThermoFisher) and stored overnight at 4 °C before storage at –80 °C until analysis.

Body condition index

Body condition index (BCI), a traditional metric used to quantify bivalve condition [17,32], calculated as $BCI = W_{dry\ tissue} / V_{shell\ cavity} \times 1000$, where $W_{dry\ tissue}$ (grams), was determined by drying the soft tissues in a pre-weighed container to a constant weight at 99 °C for 24 h [32]. Shell cavity volume ($V_{shell\ cavity}$; mL) was calculated as the total displacement volume of the whole mussel, minus the displacement volume of the open shell after removal of the soft tissues.

RNA and first-strand complementary DNA synthesis

Total RNA was extracted from 20 to 50 mg of tissue using TRIzol Reagent (Invitrogen, catalog no. 15596018; ThermoFisher) according to the manufacturer's protocol. Tissues were disrupted and homogenized with a BeadBug Microtube homogenizer (Denville Scientific). Extracted RNA was quantified using a NanoDrop One spectrophotometer (Fisher Scientific), and 1 μg of RNA was treated with deoxyribonuclease I (Amplification Grade, DNase; catalog no. 18068015, Invitrogen; ThermoFisher). To synthesize complementary DNA (cDNA), MultiScribe Reverse Transcriptase, RNase inhibitor, and random primers were used according to the manufacturer's protocol (High-Capacity cDNA Reverse Transcription kit; Applied Biosystems, catalog no. 4374966; ThermoFisher).

Gene sequences

For the purpose of developing primers for quantitative real-time polymerase chain reaction (qPCR; see following), partial sequences were generated for *ca*, *calp*, *cam*, *cs*, *hsp70*, *nka*, glyceraldehyde 3-phosphate dehydrogenase (*gapdh*),

TABLE 1: Mean water chemistry variables[a] for control conditions, 15 000, and 50 000 μatm partial pressures of carbon dioxide (pCO_2) treatments[c]

pCO_2 treatment	Temperature (°C)		Dissolved oxygen (mg/L)		pH		Alkalinity (mg/L $CaCO_3$)		$[CO_2]$ (mg/L)		pCO_2[d] (μatm)	
	Exp	Post-exp	Exp	Post-exp	Exp	Post-exp	Exp	Post-exp	Exp	Post-exp	Exp	Post-exp
Control	21.4 ± 0.1	21.7 ± 0.2	8.19 ± 0.06	7.97 ± 0.08	8.24 ± 0.03	8.42 ± 0.04	204 ± 2	413 ± 3	8.7 ± 0.4	10.1 ± 0.3	< 100	< 100
15 000 μatm	21.6 ± 0.1	22.0 ± 0.2	7.78 ± 0.11	8.00 ± 0.05	7.26 ± 0.03	8.53 ± 0.04	271 ± 4	259 ± 2	39.6 ± 2.5	10.0 ± 0.3	15 758 ± 905	< 100
50 000 μatm	21.5 ± 0.1	21.5 ± 0.1	7.78 ± 0.06	8.20 ± 0.04	6.86 ± 0.06	8.48 ± 0.06	313 ± 9	254 ± 3	88.1 ± 5.6	10.6 ± 0.4	49 271 ± 2432	< 100

[a]Temperature, dissolved oxygen, pH, alkalinity, CO_2 concentration, and pCO_2.
[b]During the 28-d exposure and 14-d post-exposure periods.
[c]Data are presented as mean ± standard error.
[d]pCO_2 values of < 100 μatm represent the lowest detectable limit of the CO_2 probe used in the present study.

elongation factor 1-α (*ef1-α*), and *18s* from cDNA synthesized from mantle tissue. Gene-specific primers (Table 2) were designed based on conserved regions of sequences from several bivalve species using Primer3plus. For *cam*, *hsp70*, and *18s*, primer forward 2 was nested within the product from primers forward 1 and reverse 1 to extend the sequence; a single set of primers was sufficient to generate a partial sequence for *ca*, *cs*, *calp*, *nka*, *gapdh*, and *ef1-α*. Primers for *ca*, *calp*, and *cam* were based on sequences from *Hyriopsis cumingii* (KF206121, JQ389857, and JQ389856, respectively). Primers for *cs* were based on conserved regions in *Atrina rigida* (DQ081727), *Laternula elliptica* (HQ186262), *Mytilus galloprovincialis* (EF535882), *Pinctada fucata* (AB290881), and *Septifer virgatus* (AB613818). Primers for *ef1-α* were based on conserved regions in *Crassostrea ariakensis* (EF502000), *Crassostrea gigas* (AB122066), *Calyptogena soyoae* (AB003719), *Chlamys farreri* (JQ278034), *Dreissena polymorpha* (AJ250733), *Modiolus americanus* (AY580265), *Mytilus californianus* (AY580262), *Mytilus edulis* (AY580270), *Mytilus galloprovincialis* (AB162021), *Nucula proxima* (AY580232), *Placopecten magellanicus* (JQ781150), *Thyasira flexuosa* (JQ781151), *Thracia villosiuscula* (JQ781152), *Solemya velum* (DQ813415), and *Yoldia limatula* (DQ813417). Primers for *gapdh* were based on conserved regions in *Azumapecten farreri* (KC573783), *C. gigas* (AJ544886), *Crassostrea virginica* (EF583608), *M. galloprovincialis* (KJ875954), *Ostrea edulis* (GQ150762), and *P. fucata* (KM816643). Primers for *hsp70* were based on conserved regions in *Argopecten irradians* (AY485261), *Argopecten purpuratus* (FJ839890), *C. farreri* (AY206871), *Corbicula fluminea* (KJ461738), *C. ariakensis* (AY172024), *C. gigas* (AF144646), *Crassostrea hongkongensis* (FJ157365), *C. virginica* (AJ271444), *Cristaria plicata* (HQ148706), *H. cumingii* (KJ123764), *L. elliptica* (EF198332), *Meretrix meretrix* (HQ256748), *Mizuhopecten yessoensis* (AY485262), *Mytilus coruscus* (KF322135), *M. galloprovincialis* (AB180909), *P. fucata* (EU822509), *Paphia undulata* (JX885711), *Pteria penguin* (EF011060), *Ruditapes philippinarum* (KJ569079), *Sinonovacula constricta* (JF748730), and *Tegillarca granosa* (JN936877). Primers for *nka* and *18s* were based on sequences from *Lampsilis cardium* (AY303383 and AF120537, respectively).

All PCR reactions were performed in the same way using an Eppendorf Mastercycler where reaction compositions (total vol 25 μL) were 2 μL cDNA, 0.2 μM primer, and 5 μL Taq 5X Master Mix (Taq 5X Master Mix, catalog no. M0258L; New England BioLabs). Cycling conditions were 95 °C (30 s), 55 °C (30 s), and 68 °C (30 s) for 38 cycles and resulting products were run on 1.5% agarose gels with ethidium bromide and extracted using a QIAquick gel extraction kit (catalog no. 28704; QIAGEN). A PCR cloning kit (catalog no. 231122; QIAGEN) and Subcloning Efficiency DH5α Competent Cells (Invitrogen, catalog no. 18265017; Life Technologies) were used to clone the PCR products following the manufacturers' protocols, with the exception that cloning reactions were scaled to 5 μL instead of 10 μL. Plasmids were extracted using a QIAprep Spin Miniprep Kit (cat. no. 27104; QIAGEN) and sequenced by the Core DNA Sequencing Facility (University of Illinois at

TABLE 2: Oligonucleotide primer sets used for gene cloning in *Lampsilis siliquoidea*

Gene	Primers (5′–3′)	Sequenced product size (bp)
ca	Forward——TCA ATA TGC CGT CCT ACC GC	954
	Reverse——CCT GGC TCT GTG TAC GTG TT	
calp	Forward——TGGCAGACCAACTAACAGAAGA	404
	Reverse——TCACTTCGACATCATCATCCTCA	
cam	Forward 1——TTG CTG AGT TCA AGG AGG CA	398
	Reverse 1——ACT CGT CAT CAT CTG CAC GA	
	Forward 2——TGA CCA ACT GAC GGA AGA ACA	
	Reverse 2——TGG CCA TCT CCG TCA ATA TCT G	
cs	Forward——TGT GCT ACA ATG TGG CAC GA	712
	Reverse——TAC CAC ACC ATC GGA CCT GA	
ef1-α	Forward——TCT CTG GAT GGC ATG GAG AC	697
	Reverse——GAT GAC TCC AAC GGC GAC AG	
gapdh	Forward——TGG ATT TGG TCG TAT CGG GC	487
	Reverse——GGT GGC TGT GTA GGC ATG GA	
hsp70	Forward 1——GAG GAC ACT CTC ATC AAG CA	671
	Reverse 1——CAT GGC TCT TTC ACC CTC AT	
	Forward 2——GAT GTT GCC CCA CTG TCT C	
	Reverse 2——TTG CTG AGA CGA CCT TTG TC	
nka	Forward——TGC CCT GGC TCG TAT CTC TA	651
	Reverse——ACC ACG TTC AGC AGC TAT GT	
18s	Forward 1——GGT TCC GCT GGT GAA TCT GA	1002
	Reverse 1——CAC GCC TGC TTT GAA CAC TC	
	Forward 2——TGT CCT GAC CTA CCT CCT GG	
	Reverse 2——CAC CAC CCA CCG AAT CAA GA	

bp = base pair; *ca* = carbonic anhydrase; *calp* = calmodulin-like protein; *cam* = calmodulin; *cs* = chitin synthase; *ef1-α* = elongation factor 1-α; *gapdh* = glyceraldehyde 3-phosphate dehydrogenase; *hsp70* = heat shock protein 70; *nka* = na^+-k^+-adenosine triphosphatase.

Urbana–Champaign). The resulting partial sequences (Table 2) were sufficient to generate primers for qPCR (see section *qPCR*).

qPCR

The relative abundance of *ca*, *calp*, *cam*, *cs*, *hsp70*, and *nka* mRNA was determined by qPCR. Primers were generated using Primer3plus for the target genes as well as the reference genes *ef1-α*, *gapdh*, and *18s* (Table 3), and their specificity was verified by sequencing the product from each primer set. To optimize reaction compositions, standard curves were generated for each primer set using cDNA pooled from individuals across treatment groups (efficiencies were > 0.92). Real-time PCR was carried out using PowerUp SYBR Green Master Mix (Applied Biosystems catalog no. A25778; ThermoFisher) and an ABI 7900HT Fast Real-Time PCR System (ThermoFisher) according to manufacturer's instructions for 10-μL reactions with a primer concentration of 0.5 μM. For all genes, cDNA was diluted 20-fold with the exception that a 20 000-fold dilution was used for *18s*. Cycling conditions were 95 °C for 15 s and 60 °C for 60 s over 40 cycles.

TABLE 3: Oligonucleotide primer sets used for quantitative real-time polymerase chain reaction[a] in *Lampsilis siliquoidea*[b]

Gene	Primers (5′–3′)	Product size (bp)
ca	Forward——CCC AAG CAG CCA TAA TTC GC	94
	Reverse——TGT GTC TGC TGT GGT ACG AC	
calp	Forward——GCG GAA CTG AGG CAC GTA AT	94
	Reverse——CGT CTC CAT CTA CAT CCG CC	
cam	Forward——TCA CCA CAA AGG AAC TGG GG	108
	Reverse——TCG TTC CAT TAC CAT CGG CA	
cs	Forward——ACG TGG ACT TCA AAC CCG AA	81
	Reverse——GCC CAC ATA CTG CTC CAA CT	
ef1-α	Forward——AGT CTG GTG ATG CTG CCA TC	108
	Reverse——GCC TCA TGT CTC TGA CTG CA	
gapdh	Forward——TCT GCT GAT GCA CCC ATG TT	109
	Reverse——CCA ATG GGG CCA AAC AGT TG	
hsp70	Forward——CTG TTG CCT ATG GAG CAG CT	72
	Reverse——GAA GGT CCT GGA CAG CTT CC	
nka	Forward——GCT TAC CTG GAG TTG GGA GG	76
	Reverse——GGA ACT GAT CCG TGG GAA GG	
18s	Forward——ATT GGA GGG CAA GTC TGG TG	99
	Reverse——CCC GAG ATC CAA CTA CGA GC	

[a]Quantitative polymerase chain reaction.
[b]See Table 2 footnote for defined abbreviations.

The NORMA-gene approach of Heckmann et al. [33] was used to normalize threshold cycle (Ct) values. For comparisons among treatment groups, normalized Ct values were expressed relative to the control pCO_2 group at 1 d of exposure using the –ΔCt method [34]. For comparisons between gill and mantle tissue, a subset of samples was assessed for *calp*, *cam*, and *ca*, and normalized Ct values were expressed relative to the gill using the –ΔCt method.

Statistical analysis

The effects of pCO_2 exposure on BCI and the mRNA abundance of target genes were assessed using a 2-way analysis of variance (ANOVA) with pCO_2 level, sampling time, and their interaction ($pCO_2 \times$ sampling time) entered into the model as fixed effects. If at least one of the main effects or the interaction was significant, a Tukey–Kramer honest significant difference post hoc test was performed. Student's *t* tests were used to assess tissue differences in the mRNA level of *ca*, *calp*, and *cam* between the gill and mantle.

For all statistical analyses, a visual analysis of fitted residuals, using a normal probability plot and/or a Shapiro–Wilk normality test, was used to assess normality. In addition, homogeneity of variances was assessed using a Levene's test, as well as a visual inspection of the fitted residuals for all 2-way ANOVA statistical analyses and a Bartlett test for all Student's *t* test statistical analyses. If either the assumption of normality or the homogeneity of variance was violated (i.e., if either the tests or visual inspections detailed above failed), data were transformed (rank, log, or square root) and run with the same parametric model, provided that assumptions were met. Statistical analyses were performed using R Ver 3.3.2 and the level of significance (α) was 0.05.

TABLE 4: Results of 2-way analysis of variance for the effects of elevated partial pressures of carbon dioxide (pCO_2) exposure on *Lampsilis siliquoidea*

Variable	Main effects	*df*	Sum of squares	*F* value	*p*
BCI	pCO_2	2	33	0.135	0.874
	Time	5	13 757	22.717	< 0.001*
	$pCO_2 \times$ time	10	945	0.780	0.648
Mantle *cs*	pCO_2	2	0.443	2.543	0.083
	Time	5	1.058	2.430	0.039*
	$pCO_2 \times$ time	10	4.331	4.974	< 0.001*
Mantle *ca*	pCO_2	2	8.05	7.143	0.001*
	Time	5	7.65	1.530	0.023*
	$pCO_2 \times$ time	10	19.49	1.949	< 0.001*
Gill *cam*	pCO_2	2	3.073	26.520	< 0.001*
	Time	5	0.892	3.078	0.012*
	$pCO_2 \times$ time	10	2.915	5.031	< 0.001*
Gill *calp*	pCO_2	2	0.623	11.220	< 0.001*
	Time	5	0.548	3.949	0.002*
	$pCO_2 \times$ time	10	1.018	3.666	< 0.001*
Mantle *calp*	pCO_2	2	0.109	0.349	0.706
	Time	5	0.947	1.209	0.310
	$pCO_2 \times$ time	10	1.329	0.848	0.583
Gill *nka*	pCO_2	2	1.406	8.027	< 0.001*
	Time	5	1.403	3.204	0.010*
	$pCO_2 \times$ time	10	3.775	4.311	< 0.001*
Mantle *nka*	pCO_2	2	0.434	7.833	< 0.001*
	Time	5	0.180	1.302	0.268
	$pCO_2 \times$ time	10	0.697	2.517	0.009*
Gill *hsp70*	pCO_2	2	4.343	46.87	< 0.001*
	Time	5	2.371	10.24	< 0.001*
	$pCO_2 \times$ time	10	5.825	12.57	< 0.001*
Mantle *hsp70*	pCO_2	2	0.071	0.328	0.721
	Time	5	0.222	0.411	0.840
	$pCO_2 \times$ time	10	1.884	1.744	0.080

*$p < 0.05$.
BCI = body condition index; *cs* = chitin synthase; *ca* = carbonic anhydrase; *cam* = calmodulin; *calp* = calmodulin-like protein; *nka* = na^+-k^+-adenosine triphosphatase; *hsp70* = heat shock protein 70.

RESULTS

Mussel BCI did not differ across pCO_2 treatments but did decline over the holding period (2-way ANOVA; Table 4). Mean BCI levels were significantly lower at 28 d of exposure and during the recovery period (49.6 ± 1.4, 48.4 ± 1.4, and 49.4 ± 2.1 for 28 d of exposure, and 7 and 14 d of post-exposure, respectively) relative to the first 7 d of the exposure period (72.1 ± 2.2, 68.0 ± 2.6, and 66.4 ± 2.6 for 1, 4, and 7 d, respectively), regardless of pCO_2 treatment.

Mantle *cs* mRNA abundance was only significantly affected by treatment with 50 000 μatm pCO_2 (Figure 1A; 2-way ANOVA, Table 4). After 7 d at 50 000 μatm pCO_2, mantle *cs* mRNA levels were 2-fold lower than in control mussels and these levels increased above control after 7 d of recovery. Mantle *cs* mRNA levels were no longer different from control after 14 d of recovery in mussels previously exposed to 50 000 μatm pCO_2.

Mantle *ca* mRNA levels were significantly affected in mussels previously exposed to elevated pCO_2, after mussels had been moved to recovery conditions (Figure 1B; 2-way ANOVA, Table 4). Mantle *ca* mRNA was significantly elevated above control levels by approximately 3-fold in mussels exposed to 50 000 μatm pCO_2 after 7 d of recovery, and in mussels exposed to 15 000 μatm pCO_2 after 14 d of recovery. Mantle *ca* mRNA levels decreased significantly over time in mussels held at control conditions (i.e., ∼ 2-fold lower at 14 d of recovery compared with 1 and 7 d of holding). Levels of *ca* mRNA were also measured in the gill; however, these levels were significantly lower than those detected in the mantle (Figure 2A; Student's *t* test: $t = -9.499$, $df = 33$, $p < 0.001$) and were too low to make comparisons among treatments.

Overall, *cam* and *calp* were differentially expressed in the gill and mantle. Levels of *cam* mRNA were significantly higher in the gill compared with the mantle (Figure 2B; Student's *t* test: $t = 9.815$, $df = 32$, $p < 0.001$), whereas *calp* mRNA levels were significantly higher in the mantle compared with the gill (Figure 2C; Student's *t* test: $t = -9.499$, $df = 33$, $p < 0.001$). Although mantle *cam* mRNA levels were too low to make comparisons among treatments, gill *cam* mRNA levels were significantly affected by pCO_2 exposure (Figure 3A; 2-way ANOVA, Table 4). In mussels exposed to 50 000 μatm pCO_2, gill *cam* mRNA levels were significantly lower than control mussels following 1 d of treatment and again during the recovery period. Levels of *cam* mRNA were not significantly affected by treatment with 15 000 μatm pCO_2, with the exception that mRNA levels were significantly elevated by approximately 2-fold at 4 d of

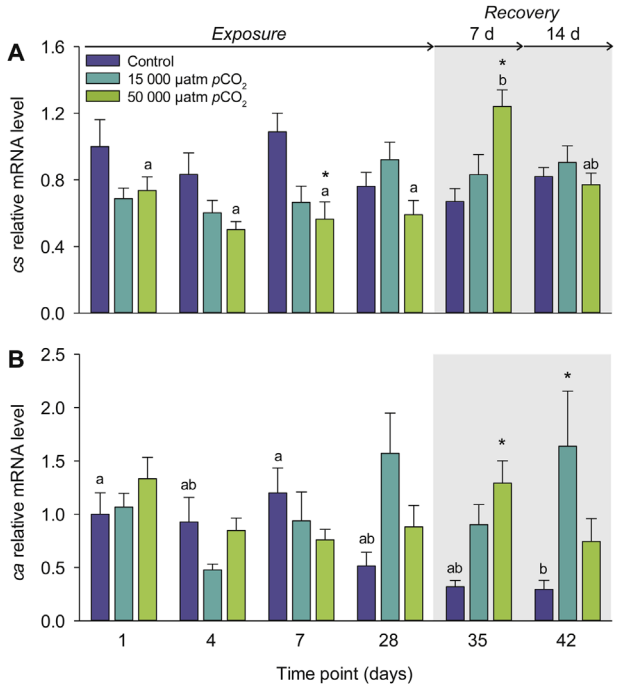

FIGURE 1: Relative mRNA levels of mantle (**A**) chitin synthase (*cs*) and (**B**) carbonic anhydrase (*ca*) in *Lampsilis siliquoidea* exposed to elevated partial pressures of carbon dioxide (pCO_2). Mussels were exposed to control conditions, 15 000, or 50 000 µatm pCO_2 for 1, 4, 7, or 28 d, and then for an additional 7 or 14 d of recovery at control conditions. Values are presented as mean ± standard error ($n = 6$–8). Levels of mRNA were measured by quantitative real-time polymerase chain reaction, and data were expressed relative to the 1-d time point from the control group. Within pCO_2 treatment groups, those not sharing a letter are significantly different from one another. Within a time point, an asterisk indicates that a treatment group is significantly different from the control group. Treatment and time effects were assessed by a 2-way analysis of variance (see Table 4 for details).

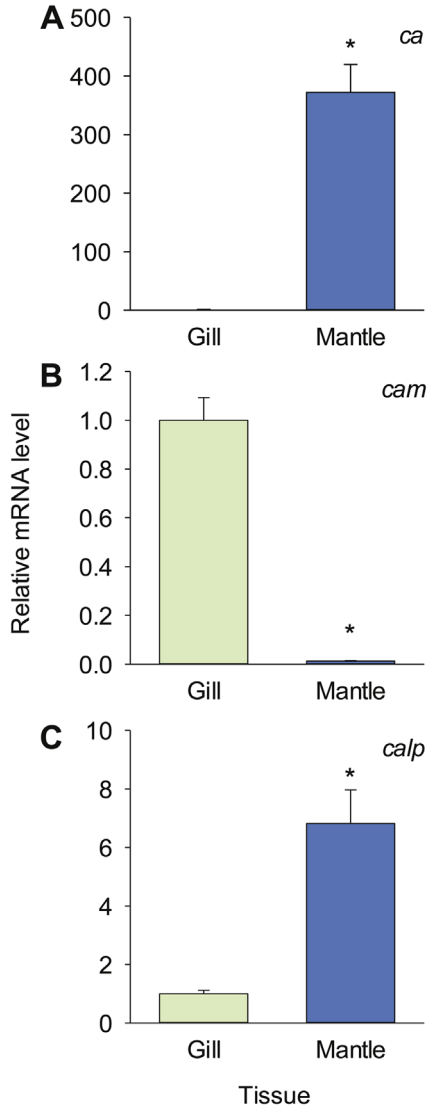

FIGURE 2: Comparison between gill and mantle (**A**) carbonic anhydrase (*ca*), (**B**) calmodulin (*cam*), and (**C**) calmodulin-like protein (*calp*) mRNA abundances in *Lampsilis siliquoidea*. Values are shown as mean ± standard error ($n = 17$–18). Levels of mRNA were measured by quantitative real-time polymerase chain reaction, and data were expressed relative to the gill (note the differences in scale along the *y* axis). An asterisk identifies a significant difference between tissues (Student's *t* test, $p < 0.001$).

treatment compared with the control and 50 000 µatm pCO_2 treatment groups. Although *calp* mRNA levels were significantly higher in the mantle compared with the gill (Figure 2C), pCO_2 treatment only had a significant effect on gill *calp* mRNA levels (Figure 3B,C; 2-way ANOVA, Table 4). In the gill, *calp* mRNA levels were significantly lower at 14 d of recovery compared with 1 d of treatment and at 7 and 14 d of recovery compared with 7 d of treatment in mussels previously exposed to 50 000 µatm pCO_2. In addition, gill *calp* mRNA levels were significantly lower in mussels treated with 50 000 µatm pCO_2 relative to the 15 000 µatm pCO_2 group at 14 d of recovery. Exposure to 15 000 µatm pCO_2 also significantly reduced gill *calp* mRNA levels by approximately 2-fold compared with the control group at 1 d of treatment but not at any other point in the treatment or recovery period. Similar to mantle *ca*, gill *calp* mRNA levels decreased with holding in the control group, with mRNA levels being lower at 14 d of recovery (i.e., 42 d of holding) compared with 7 d of holding at control conditions.

Gill and mantle *nka* mRNA levels were only affected during the recovery period in mussels previously exposed to 50 000 µatm pCO_2 (Figure 4; 2-way ANOVA, Table 4). In the gill, *nka* mRNA levels decreased significantly by approximately 2-fold during the recovery period compared with 7 and 28 d of treatment with 50 000 µatm pCO_2, and these levels were also significantly lower than the control group at 14 d of recovery. Similarly, mantle *nka* mRNA levels were significantly lower at 14 d of recovery in mussels previously exposed to 50 000 µatm pCO_2 relative to the control group.

Levels of *hsp70* mRNA were only significantly affected in gill and not mantle by treatment with elevated pCO_2 (Figure 5; 2-way ANOVA, Table 4). Gill *hsp70* mRNA levels were significantly lower in mussels exposed to 15 000 µatm pCO_2 relative to the control group at 1 and 28 d of treatment as well as during the recovery period. Within the 15 000 µatm pCO_2 treatment group, *hsp70* mRNA levels marginally increased from 1 to 4 d of treatment but remained unaffected thereafter. Similarly, gill *hsp70* mRNA levels increased in mussels exposed

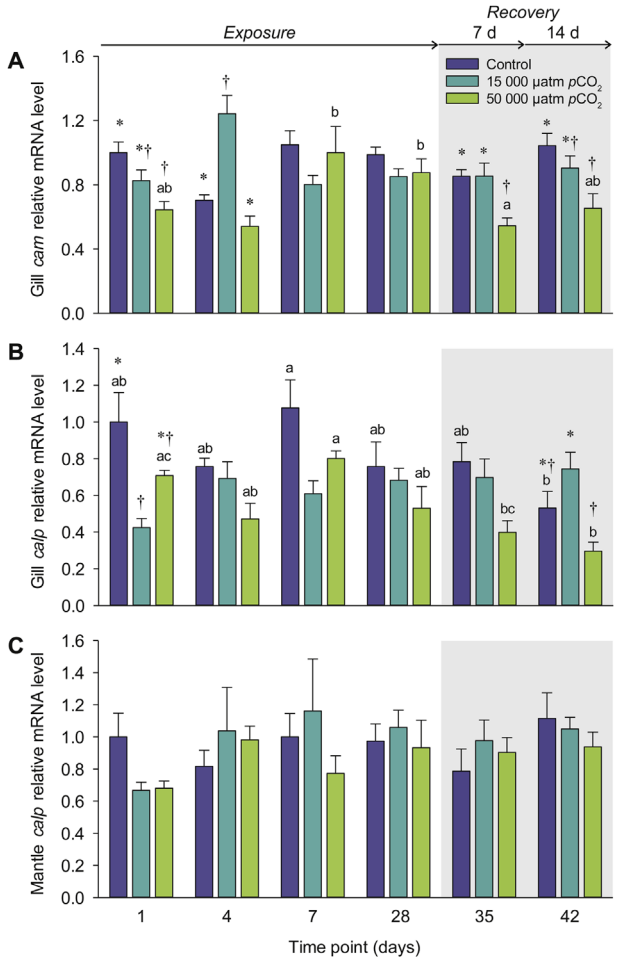

FIGURE 3: Relative mRNA levels of (**A**) gill calmodulin (*cam*), (**B**) gill calmodulin-like protein (*calp*), and (**C**) mantle *calp* in *Lampsilis siliquoidea* exposed to elevated partial pressures of carbon dioxide (pCO_2). Mussels were exposed to control conditions, 15 000, or 50 000 µatm pCO_2 for 1, 4, 7, or 28 d, and then for an additional 7 or 14 d of recovery at control conditions. Values are given as mean ± standard error ($n = 6–8$). Levels of mRNA were measured by quantitative real-time polymerase chain reaction, and data were expressed relative to the 1-d time point from the control group. Within pCO_2 treatment groups, those not sharing a letter are significantly different from one another. Within a time point, groups that do not share a symbol (i.e., asterisk or dagger) are significantly different from one another. Treatment and time effects were assessed by 2-way analysis of variance (see Table 4 for details).

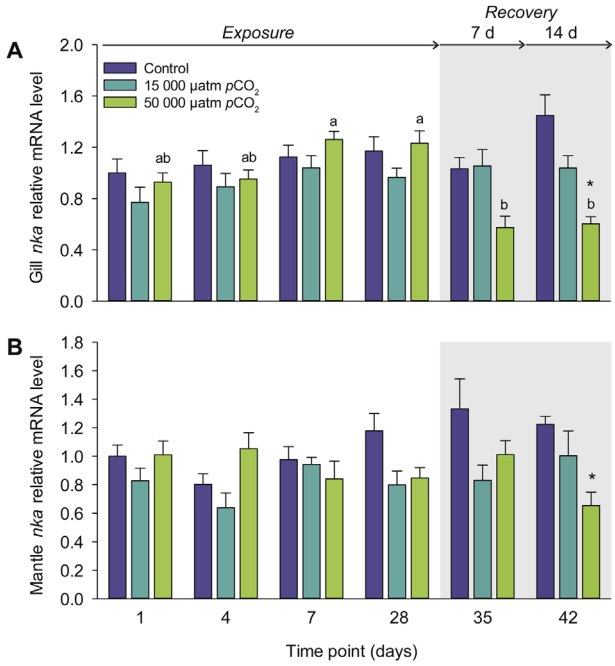

FIGURE 4: Relative mRNA levels of na^+-k^+-adenosine triphosphatase (*nka*) of (**A**) the gill and (**B**) the mantle in *Lampsilis siliquoidea* exposed to elevated partial pressures of carbon dioxide (pCO_2). Mussels were exposed to control conditions, 15 000, or 50 000 µatm pCO_2 for 1, 4, 7, or 28 d, and then for an additional 7 or 14 d of recovery at control conditions. Values are presented as mean ± standard error ($n = 6–8$). Levels of mRNA were measured by quantitative real-time polymerase chain reaction, and data were expressed relative to the 1-d time point from the control group. Within pCO_2 treatment groups, those not sharing a letter are significantly different from one another. Within a time point, an asterisk denotes that a treatment group is significantly different from the control group. Treatment and time effects were assessed by 2-way analysis of variance (see Table 4 for details).

to 50 000 µatm pCO_2 from 4 to 7 d of treatment and remained elevated until mussels were moved to recovery conditions, after which *hsp70* mRNA levels decreased below those at the onset of the treatment (i.e., 1 d) and those of mussels held at control or 15 000 µatm pCO_2. Levels of gill *hsp70* mRNA did increase marginally with holding in control mussels, where mRNA levels remained significantly elevated after 28 d of holding compared with 4 d of holding.

DISCUSSION

Several factors play a role in the biological control of shell formation in bivalves and have been shown to be sensitive to changing environmental conditions. Chitin synthase is a key enzyme in the synthesis of chitin, an insoluble polysaccharide that forms the structural framework of mollusk shells, and is important for coordination of mineralization processes and shell formation [35]. In the present study, a significant decrease in mantle *cs* mRNA was detected in *L. siliquoidea* after 7 d of exposure to 50 000 µatm pCO_2 compared with mussels held at control conditions. A similar decrease in *cs* mRNA was detected in the freshwater mussel *Fusconaia flava* exposed to 20 000 µatm pCO_2 for up to 32 d [19] and in the marine pearl oyster *P. fucata* after 72 h of exposure to approximately 900 to 2000 µatm pCO_2 [27]. Although not significant in the present study, exposure to 15 000 µatm pCO_2 also appeared to decrease *cs* mRNA levels in *L. siliquoidea* at 7 d of exposure. These decreases in the abundance of mantle *cs* mRNA may result from a decrease in the investment in shell formation. Shell formation is an energetically expensive process [36]; thus, investments in shell growth may be limited in situations where acid-base regulation is a priority, such as during exposure to elevated pCO_2. The mollusk shell is an important external structure that provides protection against predators and is used for mobility and feeding; consequently, inhibition of shell formation caused by elevations in pCO_2 could have consequences for mussel health and survival. Interestingly, mantle *cs* mRNA levels increased above those of control mussels after removal of the 50 000 µatm pCO_2 treatment. This post-exposure increase in

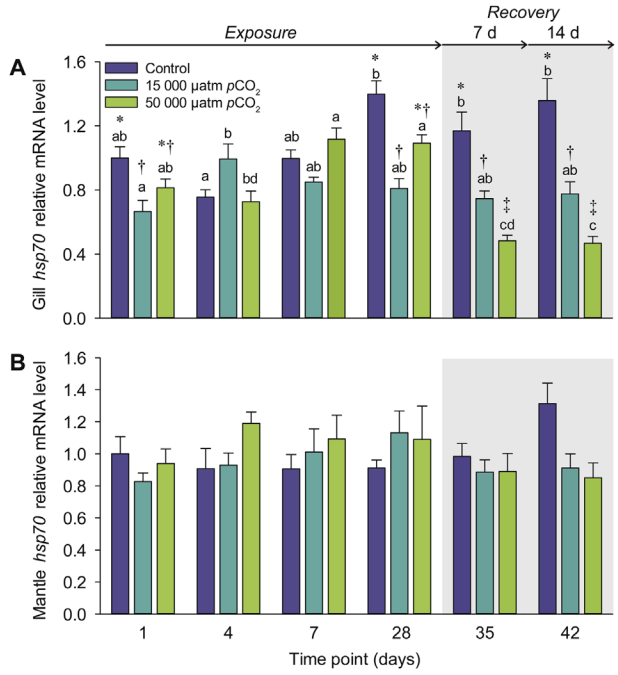

FIGURE 5: Relative mRNA levels of heat shock protein 70 (*hsp70*) of (**A**) the gill and (**B**) the mantle in *Lampsilis siliquoidea* exposed to elevated partial pressures of carbon dioxide (pCO_2). Mussels were exposed to control, 15 000, or 50 000 µatm pCO_2 for 1, 4, 7, or 28 d, and then for an additional 7 or 14 d of recovery at control conditions. Values are shown as mean ± standard error ($n = 6–8$). Levels of mRNA were measured by quantitative real-time polymerase chain reaction, and data were expressed relative to the 1-d time point from the control group. Within pCO_2 treatment groups, those not sharing a letter are significantly different from one another. Within a time point, groups that do not share a symbol (i.e., asterisk, dagger, or double dagger) are significantly different from one another. Treatment and time effects were assessed with a 2-way analysis of variance (see Table 4 for details).

mantle *cs* mRNA likely provided a compensatory mechanism for alterations in shell formation that may have occurred during pCO_2 exposure. A subsequent fall in mantle *cs* mRNA after 14 d of recovery further suggests that once the pCO_2 stressor was removed, normal shell formation may resume—as was observed in juvenile *L. siliquoidea* after 16 d post-exposure to elevated pCO_2 [20].

A similar post-recovery increase was observed for mantle *ca* mRNA abundance; however, the *ca* isoform assessed in the present study was not highly abundant in the gill. Numerous CA genes and proteins have been identified in mollusks [28,37], with CAs participating in a variety of functions related to biomineralization in the mantle [38–40], and ion transportation in the gill [41]. Although the classification and modulatory functions of mollusk CA members are increasing, they are still relatively poorly understood. In the present study, sequencing of *ca* was based on the α-*ca* (predominant CA group for metazoans) of the freshwater pearl mussel *H. cumingii* (*HcCA*), which, as in the present study, was more highly expressed in the mantle compared with the gill [42]. This pattern of expression implies that the isoform of CA investigated in the present study likely plays a specific role in regulating shell formation. In the mantle, CA provides a source of HCO_3^- for $CaCO_3$ formation by catalyzing the hydration of CO_2 to HCO_3^-, hence increasing the driving force toward biomineralization. In the present study, no effect of pCO_2 exposure on mantle *ca* mRNA was detected until the post-exposure period, where *ca* mRNA levels were elevated above those of control mussels in *L. siliquoidea* previously exposed to elevated pCO_2. Although, the effects of elevated pCO_2 on *ca* mRNA have not been previously investigated in freshwater mussels, mantle *ca* mRNA levels were sensitive to external environmental conditions in *H. cumingii*, effects that coincided with changes in shell growth and pH homeostasis [42]. Accordingly, in the present study, the post-exposure increase in mantle *ca* mRNA, similar to *cs*, may represent a compensatory response to increase biomineralization processes after exposure to elevated pCO_2. Further assessments of other potential CA isoforms, and their responses to freshwater acidification, will provide a more complete understanding of the role of CAs in regulating responses to increased pCO_2.

Calcium metabolism is another important regulator of biomineralization and includes the sequential processes of Ca^{2+} absorption, accumulation, transportation, and incorporation into the shell. Both CaM and CaM-like protein are considered important regulators of Ca^{2+} metabolism in marine bivalves [43–47]. Although calcium metabolism likely differs between freshwater and marine bivalves owing to the differences in environmental Ca^{2+} concentrations, the roles of CaM and CaM-like protein as calcium regulators have been studied to some extent in freshwater pearl mussels *Hyriopsis schleglii* [48] and *H. cumingii* [49]. In the present study, *cam* and *calp* mRNA abundance differed between the gill and mantle of *L. siliquoidea*, with *cam* mRNA being more abundant in the gill and *calp* mRNA levels being higher in the mantle. Similar transcript expression patterns of *cam* and *calp* in the gill and mantle have been found in both freshwater [48,49] and marine bivalves [43,44]. In the present study, *cam* and *calp* mRNA levels were only significantly affected by pCO_2 exposure in the gill. In bivalves, the gill is the primary location for Ca^{2+} uptake from the external environment [50,51]. After 24 h of exposure, gill *cam* and *calp* mRNA levels decreased by approximately 2-fold in response to 50 000 and 15 000 µatm pCO_2, respectively. Transcript levels of *cam* and *calp* were then relatively unaffected until the recovery period, where they fell below control levels in mussels previously exposed to 50 000 µatm pCO_2. Interestingly, this decrease in *cam* and *calp* mRNA during the recovery period coincided with lower levels of hemolymph Ca^{2+} in mussels previously exposed to elevated pCO_2 compared with control mussels [16]. If CaM and CaM-like protein are involved in gill absorption and accumulation of environmental Ca^{2+}, these data imply that a decrease in Ca^{2+} absorption may occur after exposure to a high pCO_2 in *L. siliquoidea*, which is mediated through lower levels of *cam* and *calp* mRNA; however, the reason for this decrease in Ca^{2+} absorption post-CO_2 exposure is unclear. The mantle is a key tissue responsible for the secretion of Ca^{2+} and other ions for the formation of the shell [23,52] and CaM-like protein is likely an important regulator of this highly controlled process in bivalves [43,47,53]. The high abundance of *calp* mRNA in the mantle in the present study suggests that *calp* might play an important role in shell formation in *L. siliquoidea*;

nevertheless, *calp* mRNA in the mantle did not appear to be sensitive to changes in environmental pCO_2. Expression levels of CaM-like protein are location-specific within the mantle in other bivalve species (e.g., highest in the mantle edge compared with other regions in *H. cumingii* [49]). In the present study, a combination of mantle areas was used for mRNA analysis, which may have limited the ability to detect location-specific effects of pCO_2 on *calp* mRNA. Together, these results suggest that in *L. siliquoidea* a decrease in the uptake of environmental Ca^{2+} after exposure to elevated pCO_2 may be mediated by *cam* and *calp* in the gill; nonetheless, deposition of Ca^{2+} from the mantle via a *calp*-dependent mechanism may not be affected.

The main driver of secondary active ion transport, Na^+-K^+-ATPase also provides the motive force that is necessary for Na^+ uptake. In the present study, *nka* mRNA was not significantly affected by pCO_2 exposure until the post-exposure period. Gill *nka* mRNA decreased by approximately 2-fold during the recovery period in mussels previously exposed to 50 000 μatm pCO_2 and a similar decrease was observed in the mantle following 14 d of recovery. Ion-regulatory changes were previously assessed in freshwater mussels in response to similarly high levels (20 000–55 000 μatm) of sustained [16] and intermittent [18] CO_2 exposure. In these studies, mussels showed a significant increase in hemolymph Na^+ levels in response to elevated pCO_2 that was thought to have resulted from an increase in H^+ excretion via the Na^+/H^+ exchanger, thus also increasing Na^+ uptake [54]. Hemolymph Na^+ levels subsequently decreased post-exposure in *L. siliquoidea* and *Amblema plicata* previously exposed to elevated pCO_2 [16]. The decrease in *nka* mRNA levels in *L. siliquoidea* during the recovery period in the present study may represent a decrease in Na^+ uptake during this time, allowing for Na^+ levels to decrease back to baseline (i.e., through passive loss to the freshwater environment). Interestingly, *nka* mRNA levels remained low after 14 d at control conditions, suggesting that an extended period post-CO_2 exposure may be required for recovery of ionic disturbances experienced during pCO_2 exposure. Assessments of NKA activity are required to determine whether changes in *nka* transcript abundance reflect activity level changes of this enzyme; nevertheless, a comparable decrease in whole-body Na^+ during copper exposure was thought to result from a decrease in NKA activity in juvenile *L. siliquoidea* [55]. These results suggest that *L. siliquoidea* may regulate *nka* mRNA after exposure to elevated pCO_2 to clear a Na^+ load acquired during pCO_2 exposure.

Levels of *hsp70* mRNA have been previously shown to be sensitive to changes in environmental condition in bivalves [56]. In a previous study, *hsp70* mRNA levels were significantly increased by a 32-d exposure to 20 000 μatm pCO_2 in the gill but not the mantle of the freshwater mussel *F. flava* [19]. Mantle *hsp70* mRNA levels were similarly unaltered by pCO_2 exposure in *L. siliquoidea* in the present study. Within mussels exposed to 50 000 μatm pCO_2, gill *hsp70* mRNA levels increased significantly by approximately 1.5-fold from 4 to 7 d of exposure, and remained elevated until 28 d of exposure that may represent a cellular response to the CO_2 stressor. Levels of gill *hsp70* mRNA then decreased by approximately 2-fold during the post-exposure period in mussels previously exposed to 50 000 μatm, which may have been caused by increased mRNA turnover or decreased mRNA production, although the consequences for HSP70 protein levels are unclear and warrant further investigation. The gill *hsp70* mRNA levels were also lower than those of control mussels, which may, in part, have been the result of a marginal but significant increase in *hsp70* mRNA levels in the control group over the holding period. Overall, the effect of pCO_2 exposure on *hsp70* mRNA levels was minimal in *L. siliquoidea* compared with *F. flava*, and may point to species-specific regulation of cellular components of the stress response, although a broader investigation of genes related to cellular stress is needed.

In many cases, the impacts of elevated pCO_2 exposure on the variables assessed in the present study were not evident until the post-exposure period. This delay in the assessed responses to elevated pCO_2 exposure may reflect the ability of *L. siliquoidea* to regulate during pCO_2 exposure (e.g., acid-base status), and utilize compensatory mechanisms after exposure to maintain a state of homeostasis. Alternatively, the changes that were observed in control mussels over the 42 d of holding (i.e., increase in gill *hsp70* mRNA, decrease in mantle *ca* and gill *calp* mRNA, and decline in BCI) suggest that long-term holding may also have contributed to the responses observed during the recovery period. Because of the decrease in BCI observed over the holding period, the amount of food supplied to mussels may have been insufficient; thus, in future studies, additional feeding may be necessary for these holding conditions (e.g., every day rather than every other day). However, the significant differences between mussels previously exposed to elevated pCO_2 and control mussels during the recovery period suggest that exposure to elevated pCO_2 likely still played a role in regulation of biomineralization and ion-regulatory responses in *L. siliquoidea*. Long-term holding of animals in the laboratory can be difficult; nonetheless, manipulation of the animals during the holding period was limited, mussels were provided with sediment in which to bury, and no mortality occurred. Consequently, the results of the present study are valuable and point to mechanisms that *L. siliquoidea* may utilize to regulate against acid-base and ionic disturbances experienced after exposure to elevated pCO_2.

Overall, the data from the present study provide a mechanistic understanding of the potential consequences for biomineralization and ion-regulatory processes of freshwater mussels to elevations in pCO_2. No mortality occurred over the course of the experimental period in the present study, and similar levels of pCO_2 (42 mg/L) caused low mortality in juvenile *L. siliquoidea* [20], indicating that *L. siliquoidea* were reasonably tolerant to elevations in pCO_2. However, although survival was not significantly impacted by exposure to 28 d of elevated pCO_2, sublethal impacts were evident—particularly when mussels were exposed to 50 000 μatm pCO_2 (Figure 6). During pCO_2 exposure, mussels may reduce chitin synthesis through a decrease in *cs* mRNA in the mantle that may have negative consequences for shell integrity and structure, and mussels may potentially regulate other aspects of biomineralization via the uptake of Ca^{2+} in the gill by adjustments in *cam* and *calp* mRNA (Figure 6). These decreases in factors associated with biomineralization also coincided with increases in hemolymph HCO_3^- and Na^+, which

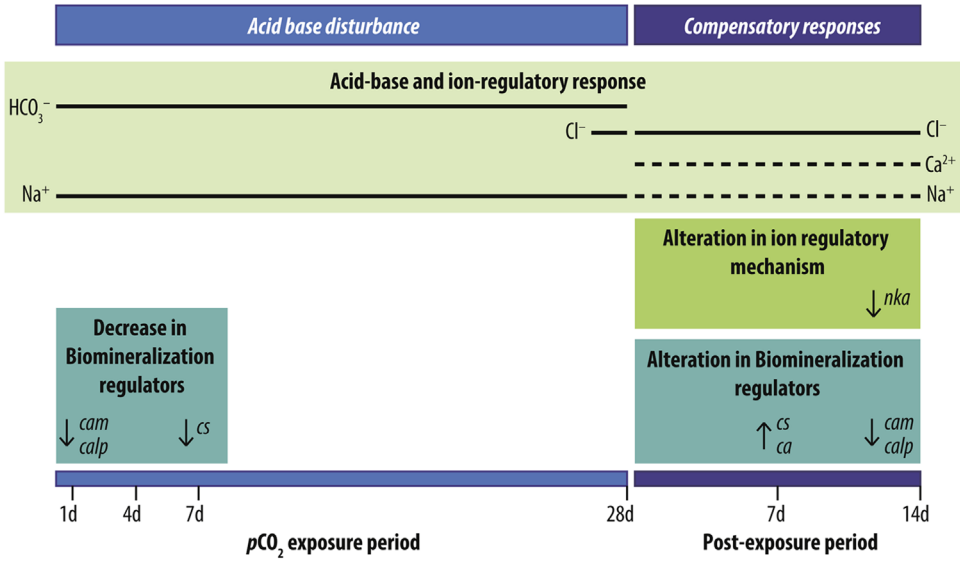

FIGURE 6: Summary of the regulatory responses during and after exposure to elevated partial pressures of carbon dioxide (pCO_2) in adult *Lampsilis siliquoidea*. Results for mussels exposed to ~ 50 000 μatm pCO_2 for a period of 1, 4, 7, and 28 d, and then for an additional 2 wk at control conditions are displayed. Factors involved in biomineralization (i.e., calmodulin [*cam*], calmodulin-like protein [*calp*], chitin synthase [*cs*], and carbonic anhydrase [*ca*]) were regulated during the first 7 d of pCO_2 exposure and during the post-exposure period. Ion-regulatory responses (i.e., na^+–k^+–adenosine triphosphatase [*nka*]) were also regulated during the post-exposure period. The compensatory reactions during the post-exposure period are likely in answer to the acid-base and ion disturbances experienced during the pCO_2 exposure period. Increases and decreases in acid-base and ion-regulatory responses (i.e., hemolymph HCO_3^-, Cl^-, Ca^{2+}, and Na^+) are represented by solid and dashed lines, respectively [16]. Note that the absence of a line for acid-base and ion-regulatory reactions indicates that hemolymph ion levels of mussels held at high pCO_2 conditions were not different from mussels held at control conditions [16].

are thought to occur in response to the release of $CaCO_3$ stores from the shell and increases in H^+ excretion via the Na^+/H^+ exchanger, respectively [16]. Thus, periods of increased pCO_2 exposure may result in a shift from an investment in shell growth to acid-base regulation caused by the intricately linked processes of calcification and acid-base regulation (i.e., carbonate buffering system). In the short term, these responses are likely to be beneficial; moreover, a decrease in shell integrity may have long-term consequences for survival in mussels because of the important protective properties of the shell. Intriguingly, freshwater mussels exhibited resilience in the compensatory responses observed during the post-exposure period. Increases in mantle *cs* and *ca* transcript abundance as well as decreases in *nka* mRNA after pCO_2 exposure may represent re-investment in biomineralization processes as well as ion regulation, respectively (Figure 6). Because many of these post-exposure responses continued to be affected even after 14 d of recovery, a longer post-exposure period (e.g., equal to or greater than the exposure period) may be necessary for full recovery from pCO_2 exposure in adult *L. siliquoidea*. Furthermore, if mussel nutrition was compromised during the exposure/post-exposure periods, this may have additionally decreased the ability of mussels to recover from pCO_2 exposure. The results from the present study have the potential to provide a foundation for the physiological responses of freshwater mussels to future increases in freshwater pCO_2 caused by both natural and anthropogenic factors. As previously indicated, the responses of freshwater bivalves to elevations in pCO_2 have been largely understudied compared with the work that has been carried out on marine bivalves in the context of ocean acidification. Although the levels of CO_2 in the present study exceed those typically used in ocean acidification studies (i.e., ~ 15 000–50 000 μatm vs ~ 800–4000 μatm for marine studies [24,27,28,30]), these levels may not be improbable for some freshwater systems [5], particularly in the case of invasive species management [14,15]. Further studies into the carry-over effects of elevated pCO_2 exposure——as well as consequences for reproduction and the role that reproductive state and sex of the mussel may play in mediating responses——would provide additional information on population level consequences for freshwater mussels exposed to high pCO_2.

Acknowledgment—The present study received support from the US Geological Survey (G14AC00119). Funding was also provided by the US Fish and Wildlife Service Federal Aid in Sport Fish Restoration Project (F-69-R), and the US Department of Agriculture National Institute of Food and Agriculture Hatch Project (ILLU-875-947). The authors thank C. Barnhart at Missouri State University for providing mussels. We are also grateful to A. Wright and J. Grandone for their valuable help with mussel husbandry and laboratory assistance.

Disclaimer—The present study is solely the responsibility of the authors and does not necessarily represent the official views of the US Geological Survey.

Data Availability—DNA sequences have been submitted to the GenBank, with accession numbers KY978468–76. Body condition index and mRNA data are available on request from the corresponding author (jjeffrey@illinois.edu).

REFERENCES

[1] Phillips J, McKinley G, Bennington V, Bootsma H, Pilcher D, Sterner R, Urban N. 2015. The potential for CO_2-induced acidification in freshwater: A Great Lakes case study. *Oceanography* 25:136–145.

[2] Zhang S, Lu XX, Sun H, Han J, Higgitt DL. 2009. Major ion chemistry and dissolved inorganic carbon cycling in a human-disturbed mountainous river (the Luodingjiang River) of the Zhujiang (Pearl River), China. *Sci Total Environ* 407:2796–2807.

[3] Barnes RT, Raymond PA. 2009. The contribution of agricultural and urban activities to inorganic carbon fluxes within temperate watersheds. *Chem Geol* 266:318–327.

[4] Noatch MR, Suski CD. 2012. Non-physical barriers to deter fish movements. *Environ Rev* 20:71–82.

[5] Cole JJ, Caraco NF. 2001. Carbon in catchments: Connecting terrestrial carbon losses with aquatic metabolism. *Mar Freshw Res* 52:101–110.

[6] Hasler CT, Butman D, Jeffrey JD, Suski CD. 2016. Freshwater biota and rising pCO_2? *Ecol Lett* 19:98–108.

[7] Doney SC, Fabry VJ, Feely RA, Kleypas JA. 2009. Ocean acidification: The other CO_2 problem. *Ann Rev Mar Sci* 1:169–192.

[8] Heuer RM, Grosell M. 2014. Physiological impacts of elevated carbon dioxide and ocean acidification on fish. *Am J Physiol Regul Integr Comp Physiol* 307:R1061–1084.

[9] Gazeau F, Parker LM, Comeau S, Gattuso J-P, O'Connor WA, Martin S, Pörtner HO, Ross PM. 2013. Impacts of ocean acidification on marine shelled molluscs. *Mar Biol* 160:2207–2245.

[10] Pörtner H. 2008. Ecosystem effects of ocean acidification in times of ocean warming: A physiologist's view. *Mar Ecol Prog Ser* 373:203–217.

[11] Vaughn CC, Nichols SJ, Spooner DE. 2008. Community and foodweb ecology of freshwater mussels. *J North Am Benthol Soc* 27:409–423.

[12] Vaughn CC. 2010. Biodiversity losses and ecosystem function in freshwaters: Emerging conclusions and research directions. *BioScience* 60:25–35.

[13] US Army Corps of Engineers. 2014. The GLMRIS Report: Great Lakes and Mississippi River interbasin study. Washington, DC.

[14] Cupp A, Erickson RA, Fredricks KT, Swyers NM, Hatton TW, Amberg JJ. 2016. Responses of invasive silver and bighead carp to a carbon dioxide barrier in outdoor ponds. *Can J Fish Aquat Sci* 74:297–305.

[15] Donaldson MR, Amberg J, Adhikari S, Cupp A, Jensen N, Romine J, Wright A, Gaikowski M, Suski CD. 2016. Carbon dioxide as a tool to deter the movement of invasive bigheaded carps. *Trans Am Fish Soc* 145:657–670.

[16] Hannan KD, Jeffrey JD, Hasler CT, Suski CD. 2016. The response of two species of unionid mussels to extended exposure to elevated carbon dioxide. *Comp Biochem Phys A* 201:173–181.

[17] Hannan KD, Jeffrey JD, Hasler CT, Suski CD. 2016. Physiological effects of short- and long-term exposure to elevated carbon dioxide on a freshwater mussel, *Fusconaia flava*. *Can J Fish Aquat Sci* 73:1–9.

[18] Hannan KD, Jeffrey JD, Hasler CT, Suski CD. 2016. Physiological responses of three species of unionid mussels to intermittent exposure to elevated carbon dioxide. *Conserv Physiol* 4:cow066.

[19] Jeffrey JD, Hannan KD, Hasler CT, Suski CD. 2017. Responses to elevated CO_2 exposure in a freshwater mussel, *Fusconaia flava*. *Comp Biochem Phys B* 187:87–101.

[20] Waller DL, Bartsch MR, Fredricks KT, Bartsch LA, Schleis SM, Lee SH. 2017. Effects of carbon dioxide on juveniles of the freshwater mussel (*Lampsilis siliquoidea* [Unionidae]). *Environ Toxicol Chem* 36:671–681.

[21] McMahon RF, Bogan AE. 2001. Mollusca: Bivalvia. In Thorp JH, Covich AP, eds, *Ecology and Classification of North American Freshwater Invertebrates*, Vol 2. Academic, New York, NY, USA, pp 331–429.

[22] Heming TA, Vinogradov GA, Klerman AK, Komov VT. 1988. Acid-base regulation in the freshwater pearl mussel *Margaritifera margaritifera*: Effects of emersion and low pH. *J Exp Biol* 137:501–511.

[23] Wilbur KM, Saleuddin ASM. 1983. Shell formation. In Saleuddin ASM, Wilbur KM, eds, *The Mollusca*, Vol 4. Academic, New York, NY, USA, pp 235–287.

[24] Hüning AK, Melzner F, Thomsen J, Gutowska MA, Krämer L, Frickenhaus S, Rosenstiel P, Pörtner HO, Philipp EER, Lucassen M. 2012. Impacts of seawater acidification on mantle gene expression patterns of the Baltic Sea blue mussel: Implications for shell formation and energy metabolism. *Mar Biol* 160:1845–1861.

[25] Melzner F, Stange P, Trubenbach K, Thomsen J, Casties I, Panknin U, Gorb SN, Gutowska MA. 2011. Food supply and seawater pCO_2 impact calcification and internal shell dissolution in the blue mussel *Mytilus edulis*. *PLoS One* 6:e24223.

[26] Michaelidis B, Ouzounis C, Paleras A, Pörtner HO. 2005. Effects of long-term moderate hypercapnia on acid-base balance and growth rate in marine mussels *Mytilus galloprovincialis*. *Mar Ecol Prog Ser* 293:109–118.

[27] Li S, Liu C, Huang J, Liu Y, Zhang S, Zheng G, Xie L, Zhang R. 2016. Transcriptome and biomineralization responses of the pearl oyster *Pinctada fucata* to elevated CO_2 and temperature. *Sci Rep* 6:18943.

[28] Wang X, Wang M, Jia Z, Qiu L, Wang L, Zhang A, Song L. 2017. A carbonic anhydrase serves as an important acid-base regulator in pacific oyster *Crassostrea gigas* exposed to elevated CO_2: Implication for physiological responses of mollusk to ocean acidification. *Mar Biotechnol* 19:22–35.

[29] Li S, Huang J, Liu C, Liu Y, Zheng G, Xie L, Zhang R. 2016. Interactive effects of seawater acidification and elevated temperature on the transcriptome and biomineralization in the pearl oyster *Pinctada fucata*. *Environ Sci Technol* 50:1157–1165.

[30] Cummings V, Hewitt J, Van Rooyen A, Currie K, Beard S, Thrush S, Norkko J, Barr N, Heath P, Halliday NJ, Sedcole R, Gomez A, McGraw C, Metcalf V. 2011. Ocean acidification at high latitudes: Potential effects on functioning of the Antarctic bivalve *Laternula elliptica*. *PLoS One* 6: e16069.

[31] Riebesell U, Fabry VJ, Hansson L, Gattuso J-P. 2010. *Guide to Best Practices for Ocean Acidification Research and Data Reporting*. The European Union, Luxembourg City, Luxembourg.

[32] Widdows J, Johnson D. 1988. Physiological energetics of *Mytilus edulis*: Scope for growth. *Mar Ecol Prog Ser* 46:113–121.

[33] Heckmann LH, Sorensen PB, Krogh PH, Sorensen JG. 2011. NORMA-gene: A simple and robust method for qPCR normalization based on target gene data. *BMC Bioinformatics* 12:250.

[34] Livak KJ, Schmittgen TD. 2001. Analysis of relative gene expression data using real-time quantitative PCR and the $2^{-\Delta\Delta Ct}$ method. *Methods* 25:402–408.

[35] Schonitzer V, Weiss IM. 2007. The structure of mollusc larval shells formed in the presence of the chitin synthase inhibitor nikkomycin Z. *BMC Struct Biol* 7:71.

[36] Palmer AR. 1992. Calcification in marine molluscs: How costly is it? *Proc Natl Acad Sci U S A* 89:1379–1382.

[37] Nielsen SA, Frieden E. 1972. Carbonic anhydrase activity in molluscs. *Comp Biochem Phys B* 41:461–468.

[38] Ebanks SC, O'Donnell MJ, Grosell M. 2010. Characterization of mechanisms for Ca^{2+} and HCO_3^-/CO_3^{2-} acquisition for shell formation in embryos of the freshwater common pond snail *Lymnaea stagnalis*. *J Exp Biol* 213:4092–4098.

[39] Istin M, Girard JP. 1970. Carbonic anhydrase and mobilisation of calcium reserves in the mantle of lamellibrachs. *Calcif Tissue Res* 5:247–260.

[40] Lopes-Lima M, Bleher R, Forg T, Hafner M, Machado J. 2008. Studies on a PMCA-like protein in the outer mantle epithelium of *Anodonta cygnea*: Insights on calcium transcellular dynamics. *J Comp Physiol B* 178:17–25.

[41] Henry RP, Saintsing DG. 1983. Carbonic anhydrase activity and ion regulation in three species of osmoregulating bivalve molluscs. *Physiol Zool* 56:274–280.

[42] Ren G, Wang Y, Qin J, Tang J, Zheng X, Li Y. 2014. Characterization of a novel carbonic anhydrase from freshwater pearl mussel *Hyriopsis cumingii* and the expression profile of its transcript in response to environmental conditions. *Gene* 546:56–62.

[43] Li S, Xie L, Ma Z, Zhang R. 2005. cDNA cloning and characterization of a novel calmodulin-like protein from pearl oyster *Pinctada fucata*. *FEBS J* 272:4899–4910.

[44] Li S, Xie L, Zhang C, Zhang Y, Gu M, Zhang R. 2004. Cloning and expression of a pivotal calcium metabolism regulator: Calmodulin involved in shell formation from pearl oyster (*Pinctada fucata*). *Comp Biochem Phys B* 138:235–243.

[45] Li S, Xie L, Meng Q, Zhang R. 2006. Significance of the extra C-terminal tail of CaLP, a novel calmodulin-like protein involved in oyster calcium metabolism. *Comp Biochem Phys B* 144:463–471.

[46] Fang Z, Yan Z, Li S, Wang Q, Cao W, Xu G, Xiong X, Xie L, Zhang R. 2008. Localization of calmodulin and calmodulin-like protein and their functions in biomineralization in *P. fucata*. *Prog Nat Sci* 18:405–412.

[47] Yan Z, Fang Z, Ma Z, Deng J, Li S, Xie L, Zhang R. 2007. Biomineralization: Functions of calmodulin-like protein in the shell formation of pearl oyster. *Biochim Biophys Acta* 1770: 1338–1344.

[48] Zeng LG, Wang JH, Li YJ, Sheng JQ, Gu Q, Hong YJ. 2012. Molecular characteristics and expression of calmodulin cDNA from the freshwater pearl mussel, *Hyriopsis schlegelii*. *Gen Mol Res* 11:42–52.

[49] Ren G, Hu X, Tang J, Wang Y. 2013. Characterization of cDNAs for calmodulin and calmodulin-like protein in the freshwater mussel *Hyriopsis cumingii*: Differential expression in response to environmental Ca^{2+} and calcium binding of recombinant proteins. *Comp Biochem Phys B* 165:165–171.

[50] Rousseau M, Plouguerné E, Wan G, Wan R, Lopez E, Fouchereau-Peron M. 2003. Biomineralisation markers during a phase of active growth in *Pinctada margaritifera*. *Comp Biochem Phys A* 135:271–278.

[51] Stommel EW. 1984. Calcium activation of mussel gill abfrontal cilia. *J Comp Physiol A* 155:457–469.

[52] Suzuki M, Nagasawa H. 2013. Mollusk shell structures and their formation mechanism. *Can J Zool* 91:349–366.

[53] Fang Z, Cao W, Li S, Wang Q, Li C, Xie L, Zhang R. 2008. Significance of the C-terminal globular domain and the extra tail of the calmodulin-like protein (*Pinctada fucata*) in subcellular localization and protein-protein interaction. *Cell Biol Int* 32:920–927.

[54] Byrne RA, Dietz TH. 1997. Ion transport and acid-base balance in freshwater bivalves. *J Exp Biol* 200:457–465.

[55] Jorge MB, Loro VL, Bianchini A, Wood CM, Gillis PL. 2013. Mortality, bioaccumulation and physiological responses in juvenile freshwater mussels (*Lampsilis siliquoidea*) chronically exposed to copper. *Aquat Toxicol* 126:137–147.

[56] Fabbri E, Valbonesi P, Frazellitti S. 2008. HSP expression in bivalves. *Invert Surviv J* 5:135–161.

